Publisher	: John Wiley & Sons, Inc.
Location	: Hoboken, USA
DOI	: 10.1002/(ISSN)1097-4628
ISSN (print)	: 0021-8995
ISSN (electronic)	: 1097-4628
ID (product)	: APP
Title (main)	: Journal of Applied Polymer Science
Title (short)	: J Appl Polym Sci
Copyright (publisher)	: © 2019 Wiley Periodicals, Inc.
Numbering (journalVolume)	: 9999
Numbering (journalIssue)	: 9999
DOI	: 10.1002/app.48448
ID (unit)	: APP48448
ID (society)	: app.20191147
ID (eLocator)	: e48448
Count (pageTotal)	: 12
Title (articleCategory)	: Article
Title (tocHeading1)	: Articles
Copyright (publisher)	: © 2019 Wiley Periodicals, Inc.
Event (manuscriptReceived)	: 2019-05-03
Event (manuscriptAccepted)	: 2019-08-10
Event (xmlCreated)	: 2019-08-22 (SPi Global)
Numbering (pageFirst)	: n/a
Numbering (pageLast)	: n/a
Object Name (figure)	: Scheme
Link (toTypesetVersion)	: file:app48448.pdf
Link (toAuthorManuscriptVersion)	: file:app48448_am.pdf

Short Title: Original antifouling strategy: Polypropylene films modified with chitosan-coated silver nanoparticles

Original antifouling strategy: Polypropylene films modified with chitosan-coated silver nanoparticles

<<Query: Please confirm that given names (blue) and surnames/family names (vermilion) have been identified and spelled correctly. Ans: It is OK.>>Giuliana<<Query: Please check if link to ORCID is correct. Ans: Mosconi´s ORCID IDhttps://orcid.org/0000-0003-3161-6425>> Mosconi[1,2], María Fernanda Stragliotto[1,2], Walter Slenk[1], Laura Elisa Valenti[3,4], Carla Eugenia Giacomelli[3,4], Miriam Cristina Strumia[1,2], Cesar Gerardo Gomez*[1,2]

[1] Departamento de Química Orgánica, Universidad Nacional de Córdoba, Facultad de Ciencias Químicas, (5000) Córdoba, Argentina

[2] Departamento de Fisicoquímica, Universidad Nacional de Córdoba, Facultad de Ciencias Químicas, (5000) Córdoba, Argentina

[3] Consejo Nacional de Investigaciones Científicas y Técnicas (CONICET), Instituto de Investigación en Fisicoquímica de Córdoba (INFIQC), (5000) Córdoba, Argentina

[4] Consejo Nacional de Investigaciones Científicas y Técnicas (CONICET), Instituto de Investigación y Desarrollo en Ingeniería de Procesos y Química Aplicada (IPQA), (5000) Córdoba, Argentina

Cesar Gerardo Gomez: ✉ gom@fcq.unc.edu.ar

Correspondence to: Correspondence to: C. G. Gomez (E-mail: gom@fcq.unc.edu.ar)

FundRef Name	FundRef Organization Name	Funding Number
SeCyT-UNC		30820150100348CB
FONCYT	Fondo para la Investigación Científica y Tecnológica	PICT-2015-2477
CONICET	Consejo Nacional de Investigaciones Científicas y Técnicas	PIP 11220150100344CO, 11220110100499CO

ABSTRACT

A new coating strategy of polypropylene (PP) films with silver nanoparticles (AgNPs) is proposed to obtain surfaces with antifouling properties. As a first step, the photograft polymerization is used to produce polyacrylic acid-grafted PP (PAA-grafted PP) films. A green AgNP synthesis is used by thermal reduction of $AgNO_3$ with amino groups of chitosan (CS), which controls ion diffusion and stabilizes nanoparticles. AgNP/CS complexes are adsorbed on PAA-grafted PP by electrostatic interactions, yielding AgNP/CS-coated PP films. These films show an excellent antimicrobial activity, even for AgNP contents as low as 0.08 wt %, reducing more than 4 log units in the viable *Staphylococcus aureus* concentration or inducing *Escherichia coli* death. This trend is consistent with an adequate amount of small AgNP adsorbed in an organized manner within a thin surface layer. Therefore, the antimicrobial activity of this film seems to be more than promising, used as an active surface for a wide range of applications.

Graphical Abstract

A new coating strategy to obtain surfaces with antifouling properties is proposed. Polyacrylic acid-grafted polypropylene films were used to adsorb silver nanoparticles (AgNP/CS) complexes obtained from thermal reduction of silver ions in the presence of CS. Then, AgNP/CS-coated PP films showed an excellent antimicrobial activity against Staphylococcus aureus *and* Escherichia coli, even for AgNP contents as low as 0.08 wt %.

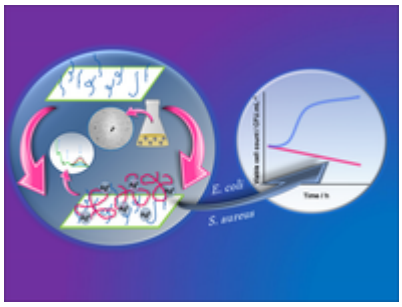

Keywords: coatings; nanocrystals; nanoparticles; nanowires; packaging; photopolymerization; surfaces and interfaces

Figure S.1 AA-Photograft polymerization onto surface of PP films. (Left) Performance of G value and thickness of PAA-grafted PP films obtained and their (Right) absorbance band ratio ($A_{1712\ cm\text{-}1}$/ $A_{1456\ cm\text{-}1}$) when different BP concentrations in the reaction mixture were used for 30 seconds of exposure time against UV light.

Figure S.2. SEM micrographs from secondary (left) or backscattered electrons (right) corresponding to the surface of $AgNP^5$/CS-coated PP (up and medium) and $AgNP^{30}$/CS-coated PP film (down) with a I value near 1.4 wt%. These films were obtained from adsorption of AgNPx/CS complexes onto PAA-grafted PP films (G = close to 2 wt%). A magnification of 5 (up) and 100 kX (medium and down) is shown into micrographs.

Figure S.3. (A) UV–Visible spectral curves of sodium 4-nitrofenoxide, whose reduction kinetics for 60 (gray), 180 (orange), 300 (magenta), 420 (light blue), 540 (blue), 660 (light green), 780 (red) and 1200 seconds (black) were performed at 50°C. (B) Variation of sodium 4-nitrofenoxide extinction corresponding to its reduction kinetics for $AgNP^{30}$/CS-coated PP film determined at 400 nm. $AgNP^{30}$/CS-coated PP film has a I value near 1.4 wt% and was obtained from a PAA-grafted PP film with a 2 wt% of G value.

Figure S.4. Inhibition diameter generated by PP (1), PAA-grafted PP^a (2), CS-adsorbed PP^b (3), $AgNP^5$/CS-coated PP^b (4) and $AgNP^{30}$/CS-coated PP^b (5) film after 24 hours of *S. aureus* (left) and *E. coli* (right) growth at 37°C. (a) PAA-grafted PP film with a G value of 2 wt%. (b) These films have a I value near 1.4 wt.-% and were obtained from PAA-grafted PP^a.

Scheme S.1. AA photograft polymerization on PP film.

Table S.1. Logarithmic reduction on the viable cell content (CFU/mL) of *S. aureus* (left) and *E. coli* (right) calculated from Figure 7 data for AgNP/CS-coated PP films. Initial inoculum concentration: 10^3 CFU/mL.

Table S.2. Logarithmic reduction on the viable cell content (CFU/mL) of *S. aureus versus* incubation time calculated for AgNP/CS-coated PP films described in Table S.1. Initial inoculum concentration: 10^6 CFU/mL.

INTRODUCTION

Chitosan (CS) is a linear polysaccharide composed of randomly distributed β-1,4-D-glucosamine and N-acetyl-D-glucosamine, obtained by deacetylation of chitin.[1] This polysaccharide has been widely used as a packaging precursor due to its high film-forming capacity.[2] However, CS films are brittle with poor mechanical properties.[3] Therefore, the synthesis of biocomposite materials prepared from the combination of a synthetic polymer with high mechanical and chemical stability and low-cost production,[4–8] such as

polypropylene (PP), and a biopolymer like chitosan (CS), has been extensively used. In addition, as PP requires appropriate properties to be used for a specific application, for example, a given functionality, the portion that comes in contact with the environment must be modified.[9] *Thus, the* changes should occur only in a shallow depth from the surface, without modifying the properties of the polymer bulk.[10] The superficial modification of polymers has been a significant subject over several decades.[11, 12] Among the techniques implemented, surface graft has several advantages comprising easy and controllable degree of grafted chains, which allows reaching a *layer boundary* between the bulk polymer and the outer environment.[13] In addition, the covalent attachment of the grafted chains on the surface of a polymer prevents desorption, ensuring the long-term chemical stability of the grafted chains.[14] Different synthetic routes can be used to introduce grafted chains into the system of interest. There are two graft systems generally used: "graft-from" or "graft-to".[15, 16] Graft-from reaction involves the use of active species on the surface of the polymer to initiate the polymerization of the monomers from the surface.[17, 18]

A suitable combination of a natural and a synthetic polymer improves the properties of the resulting material, which expands its application field. This methodology of synthesis has proved to be appropriate in areas such as biomedical materials, controlled release systems, biological tissue engineering and packaging, food packaging.[19–23]

The antimicrobial activity can be imparted to materials employing compounds that reduce or inhibit the growth of microorganisms, without showing general toxicity in the surroundings of the treated center.[24–27] The antibacterial agents (antibiotics) most commonly used come from completely natural products, such as aminoglycosides; chemically modified natural compounds, such as penicillin, cephalosporin, or carbapenem; and completely synthetic ones, such as sulfonamides.[28–32] However, the widespread use of these substances and their abuse have led, in many cases, to bacterial resistance, a growing issue that calls for the development of new strategies.[33–35] In addition, it is known that traditional antibiotics are little or almost not efficient against bacterial biofilm formation. In this scenario, the implementation of nanotechnology has been proposed for a more effective control of bacterial development based on their capacity for cell penetration.[36, 37] In that sense, silver nanoparticles (AgNPs) have a powerful antimicrobial activity of broad spectrum, effective against the development of biofilms.[38–40] In recent years, the synthesis of noble metal nanoparticles (NPs) has also drawn attention due to their particular properties, which enable their application in numerous fields.[41–43] However, the use of NP is often limited due to their colloidal instability, whereby stabilizing agents such as polymers have been incorporated to prevent their aggregation.[15, 44] Generally, the NPs are produced by the chemical reduction of solubilized metal ions in the presence of a reducing agent. Taking advantage of the chemical structure of CS, Wei *et al.* synthesized AgNP in aqueous solution from the thermal reduction of silver ions where the amine group of the polysaccharide was an effective reducing and a stabilizing agent.[45, 46] Additionally, it was found that an increase in silver ion concentration in the reaction mixture (RM) containing CS led to the formation of a higher AgNP content. Based on these results, we hypothesize that the silver ion content could also govern the size of the AgNP formed. It should be noted here that it is known that AgNP have a certain cytotoxicity level, so their wide use in biomedical and food materials is still under study.[38] Yet, Shao *et al.* showed, in a similar study,[47] that the cytotoxicity of AgNP deposited on the film surface was substantially reduced compared with the same concentration of free AgNP. This behavior was highly encouraging for the development of active antimicrobial surfaces containing these metal NP. Therefore, this work aimed at preparing PP films with antimicrobial activity and antifouling properties. To this end, a coating strategy of the PP surface with AgNP was proposed, using photograft polymerization of acrylic acid (AA) to incorporate the AgNP/CS complex.

EXPERIMENTAL

Materials and Equipment

The following reagents were purchased and used: commercial CS, CAS 9012-76-4 low-molecular-weight compound (50–190 kDa based on viscosity) with 85% of deacetylated degree (Aldrich<<Query: Please provide the name and location of the manufacturer (city and state in the United States and city and country elsewhere),

wherever applicable. Ans: ...(Sigma - Aldrich, USA); .....>>); near 17-μm-thick PP films (Coverflex S.A., Argentina); AA (Merck, Germany) by distillation under reduced pressure was purified; and benzophenone (BP) p.a. (Mallinckrodt). $AgNO_3$ p.a. (Prodesa S.C.A., Argentina); $NaNO_3$p.a (J. T. Baker Chemical Co.); H_2O_2 100 vol (Cicarelli, Argentina), glacial acetic acid (Cicarelli, Argentina); LIVE/DEAD BacLight Bacterial Viability Kit (L-13152) (Invitrogen). Sample characterization by ultraviolet (UV)–Visible spectroscopy was performed with a spectrophotometer Shimadzu UV-1800, Japan. In addition, the initial PP and the modified PP film were superficially characterized by FTIR spectroscopy. Attenuated total reflectance (ATR) spectra were recorded with a Thermo Scientific Nicolet iN10 FTIR spectrometer. A zinc selenide ATR crystal at 45° was used within a wavenumber range of 4000–600 cm^{-1} at 4 cm^{-1} resolution for 16 scans with Omnic 8 (Nicolet) data processing.

Film thickness was determined using a thickness gauge (Schwyz, Switzerland) at least eight times for each sample. AgNP samples produced from the thermal reduction of silver ions were characterized by transmission electron microscopy (TEM) using a JEOL-JEM 1200 EXII instrument. Here, one drop of a diluted AgNP suspension sample was seeded twice on the copper grid of the sample holder, and then dried at 25 °C. AgNP size distribution was determined by using at least five TEM photomicrographs for each sample. A field-emission scanning electron microscope for nanometric characterization was used (SIGMA HD-ZEISS, Germany). Surface topography of modified films was evaluated from pixel values obtained from SEM photomicrographs recorded by the backscattered electron detector. These pictures were edited using the software “Image J 1.4g” (Plugin—Interactive 3D surface plot v2.22), Wayne Rasband, National Institue of Health. The visualization of the stained samples was performed using an Olympus FV300 Confocal Fluorescence microscope.

Bacterial Strains, Culture Medium, and Stain

Staphylococcus aureus ATCC 25923 and *Escherichia coli* ATCC 25922 were kindly provided by Dr. Claudia Sola (CIBICI-CONICET, Universidad Nacional de Córdoba, Córdoba, Argentina). The culture media were Tryptone Soy Agar (TSA), Tryptone Soy Broth (TSB), and Mueller-Hinton Agar (MHA), (Britannia & Co, UK). The LIVE/DEAD BacLight Bacterial Viability Kit (L-13152) was employed to visualize the bacteria adhered to the solid substrates and, thus, discriminate between live and dead bacteria by fluorescence confocal microscopy. The kit uses a mixture of the nucleic acid stain SYTO 9 (green-fluorescent) and propidium iodide (red-fluorescent). Bacteria with intact cell membranes stain fluorescent green, whereas bacteria with damaged membranes stain fluorescent red. The optimized concentration of each dye was 0.0006 mM SYTO 9 stain and 0.003 mM propidium iodide. Stock cultures of *S. aureus* ATCC 25923 and *E. coli* ATCC 25922strain were kept at 4 °C on TSB for antimicrobial assays. Microorganisms were grown overnight in TSA before performing antimicrobial assays. These cultures were used to obtain the appropriate inoculum culture for each assay. For agar disk diffusion, CLSI protocol was used.[48]

Preparation of 1.0-wt % CS Aqueous Solution

This biopolymer was solubilized under stirring at room temperature in a 0.10 M of acetic acid buffer at pH 4.0 in order to reach a 1.0 wt % of CS aqueous solution.[49, 50] A pH value lower than 4.0 leads to the hydrolysis of CS backbone, while it is insoluble at a pH greater than 5.0. This mixture was stirred for 2 h until virtually no undissolved solid was observed.

Synthesis of AgNP by Thermal Reduction of Silver Ions

Reduction reaction of silver ions against amino groups of CS took place as the RM was thermally processed (Scheme 1, step 1). AgNP synthesis was carried out from the mixing of 20.0 mL of $AgNO_3$ aqueous solution (5 or 30 mM) and 50.0 mL of a 1.0 wt % of CS aqueous solution in a capped candy-colored flask. Later, this RM was stirred for 15 min at 25 °C, and then quickly immersed in a thermostatic bath at 90 °C for 15 h. Finally,

the RM was centrifuged at 5000 rpm to remove insoluble byproducts. The colloidal suspension of AgNP/CS obtained from a 5 or 30 mM of $AgNO_3$ aqueous solution was named $AgNP^x$/CS, where x = 5 or 30.

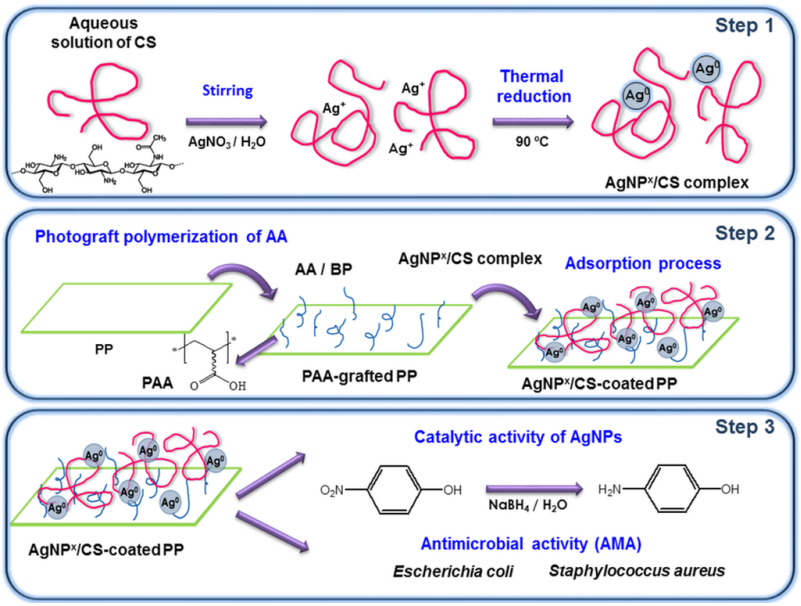

Scheme 1 Coating strategy of PP films with AgNP. Synthesis of AgNP/CS complex (Step 1), AA-photograft polymerization, and adsorption of AgNP/CS complex (Step 2). Evaluation of AgNP/CS-coated films (Step 3).

Determination of AgNP Content from Potentiometric Assays

The content of AgNP in RM was determined with a potentiometric assay at 25 °C using a silver-selective electrode (9416BN, Thermo Scientific Orion), a reference electrode (900 200, Thermo Scientific Orion), and a digital potentiometer (Mettler Toledo, Seven Compact, Switzerland). The AgNP content in the RM was calculated by the difference between the silver ion concentration before and after thermal treatment.[44] This determination was performed at least twice for each sample.

AA-Photograft Polymerization on PP Films

PP films were modified by photograft polymerization of AA, using different conditions such as reaction time, concentration of AA, and radical initiator BP to prepare PP films grafted with polyacrylic acid grafted-polypropylene (PAA-grafted PP) (Scheme 1, step 2). Rectangular PP films of 6 cm × 20 cm were modified by a photograft polymerization of AA, using BP as a photoradical initiator (Scheme S.1); 0.60 mL of RM, containing 0.10 M of BP and 3.0 M of AA aqueous solution, was deposited on a glass and then covered with a PP film (120 cm^2). The PP/RM/glass system was subsequently placed inside a photoreactor at 20 cm of distance (UV irradiance near 12 w m^{-2}) from a UV lamp centered on top. This light source (NNI 40/20 35 W, UV Consulting Peshl, Spain) has a length of 25 cm with a UV total power 188 W m^{-2} determined using a measurement method developed in our research team.[51] The reaction starts when the UV light (254 nm) passes through the PP film, which interacts with the BP molecule close to the PP surface. This molecule is activated by interaction with UV light, which works as a radical initiator of the reaction. In this study, several exposure times of the system (15, 30, 45, 60, or 75 s) were used against radiation.

After reaction was completed, the film was first purified by repeated washing with an alkaline solution of 0.1 M NaOH to remove the remaining monomer and the soluble PAA homopolymer. The excess of NaOH was removed afterward from the PAA-grafted PP film by washing with a 0.1 M of HCl aqueous solution, and then washed with distilled water until reaching neutral pH.

The modified films were dried under reduced pressure until reaching constant mass. After that, the degree of PAA grafting (*G*) on the surface of PP was calculated by eq. (1):

$$G \Big/ \text{wt \%} = \left(1 - \frac{\text{PP}}{\text{PAA} - \text{grafted PP}}\right) x\ 100 \tag{1}$$

where PP and PAA-grafted PP correspond to the mass of pristine PP and the modified PP film, respectively. This parameter was calculated from at least four PAA-grafted PP films synthesized under a given reaction condition.

Adsorption of AgNP/CS Complex onto Surface of PAA-Grafted PP Films

Successively, the AgNP/CS complex was adsorbed onto PAA-grafted PP from electrostatic interactions (Scheme 1, step 2). The adsorption of the $AgNP^x$/CS complex onto PAA-grafted PP films with different *G* values took place under light protection for 15 h at 25 °C using a similar procedure described by Cavallo *et al.*[52] In all the cases, the adsorption process took place once 1.20 mL of $AgNP^x$/CS complex colloidal suspension was left in contact with the modified face of PAA-grafted PP film (60 cm^2) to obtain a $AgNP^x$/CS-coated PP film. Then, it was washed with a 5 wt % of ammonium hydroxide aqueous solution and distilled water until reaching pH 6.0. Finally, the $AgNP^x$/CS-coated PP film was dried under reduced pressure. The immobilization degree (I) of the $AgNP^x$/CS complex onto PAA-grafted PP films was determined from eq. (2):

$$I \Big/ \text{wt \%} = \left(1 - \frac{\text{PAA} - \text{grafted PP}}{\text{AgNP}^x \Big/ \text{CS} - \text{coated PP}}\right) x\ 100 \tag{2}$$

where PAA-grafted PP and $AgNP^x$/CS-coated PP films correspond to the mass of both PP films modified, respectively. The *I* value was determined from at least four $AgNP^x$/CS-coated PP films prepared under these reaction conditions.

In parallel, experiments without AgNP were performed with a 0.71 wt % of CS aqueous solution used for adsorption onto the PAA-grafted PP (CS-adsorbed PP) films employing a similar procedure to that described above.

Finally, AgNP-coated PP films were evaluated regarding the catalytic activity of adsorbed AgNP and antimicrobial performance (Scheme 1, step 3). These two responses are complementary, since the first one is related to the AgNP surface available to the environment while the other one shows its effect against bacteria adhesion and surface colonization.

Catalytic Activity of Adsorbed AgNP

In order to assess the catalytic performance of the active surface of $AgNP^x$/CS-coated PP films, a model reaction such as the 4-nitrophenol reduction was examined. This reaction was carried out under pseudofirst-order conditions, using a molar ratio of 100 from $NaBH_4$ to 4-nitrophenol. The reduction reaction of 4-nitrophenol was developed in a sample cell for UV–Vis spectrophotometry, where 10.0 mg of a $AgNP^x$/CS-

coated PP film was left in contact with 1.00 mL of a 0.10 mM of 4-nitrophenol solution for a period of 10 min in order to wet the surface of the film where the AgNPs were adsorbed. In addition, a 20 mM of $NaBH_4$ aqueous solution was prepared just before being incorporated (2.00 mL) into the reaction. The acquisition of the spectral curve of the substrate was recorded as a function of time in the range of 200–600 nm. This study was conducted with a water bath at 50 °C, connected to the UV–Vis spectrophotometer's cell holder device.

Antimicrobial Performance of PP Films Modified with AgNP

Agar Disk Diffusion Assay

Antimicrobial activity of PP-based films was evaluated using an *in vitro* assay such as agar disk diffusion assay, a method widely used to evaluate this kind of materials.[53] Petri plates containing MHA were inoculated with a 10^8 CFU/mL of *S. aureus* or *E. coli* with a sterile swab. After that, disks of 0.40-cm diameter of PP, PAA-grafted PP (G = 2 wt %), CS-adsorbed PP (near 1.4 wt % of I value), and $AgNP^5$/CS-coated and $AgNP^{30}$/CS-coated PP films were placed onto agar surface. The CS-adsorbed film was added as a proper control in order to evaluate the antimicrobial performance of AgNP without possible interference of CS. The Petri dishes were incubated for 24 h at 37 °C. Following the incubation process, the diameter of the clear zone formed around the film disk was determined at least 10 times and reported as a qualitative measurement. In this work, an antimicrobial activity index (AMI) was calculated from eq. (3):

$$\text{AMI}\left/\ \%\ = \frac{(d_1 - d_0)}{d_1} x\ 100 \right. \tag{3}$$

where d_1 is the diameter of final halo zone and d_0 is the diameter of circular film.[54]

Growth and Viability of Planktonic Bacteria—Surface Colonization

Disks with a 1.20-cm diameter for PP, PAA-grafted PP, CS-adsorbed PP, and $AgNP^5$/CS-coated and $AgNP^{30}$/CS-coated PP films were independently placed in a 24-well plate. Then, an inoculum of 10^3 or 10^6 CFU/mL of *S. aureus* in TSB was added in each well and incubated for different times (3, 6, 24, and 48 h) at 37 °C. Proper controls were conducted with TSB in the absence of the films. After incubation, the viable cell concentration in contact with the films was quantified in the supernatant by serial dilution and counting method. This assay was performed at least twice for each plate. In addition, the films incubated with *S. aureus* for 48 h were washed with 0.90 w/v % of NaCl aqueous solution to remove nonadhered bacteria so as to evaluate surface colonization. These films were then stained with 200 μL of dye solution (as previously detailed) and incubated in the dark for 15 min. The visualization of the stained samples was performed by an Olympus FV300 Confocal Fluorescence microscope.

It is important to highlight that during the characterization of the different samples, the value of a given parameter was informed as the average value and its standard deviation, which was calculated from the measurement of at least two determinations.

RESULTS AND DISCUSSION

AA Photograft Polymerization on PP Film

UV-induced grafting of AA onto the PP surface was analyzed by following the *G* value and thickness along the exposure time. First, the radical initiator of the RM, BP, after exposure to UV light was activated (BP*) (Scheme S.1). In the second step, BP* abstracts a hydrogen atom from the PP backbone, generating a new active radical (BPH). Finally, the substituent BPH was displaced and the addition of AA monomer onto PP backbones took place.[52, 55] During this reaction, a fraction of the monomers was involved in the AA-photograft polymerization onto the PP chains, while the rest of monomers produced free PAA backbones by homopolymerization in the bulk or no reacted.

Figure 1 shows the *G* value and thickness for AA photograft polymerization as a function of exposure time. It can be observed that the photograft reaction initially shows an induction period associated with the slowdown of the polymerization. Here, the rate of BP hydrogen abstraction on PP chains is limited, since a minimum concentration of activated BP is required to reach a suitable photograft polymerization rate (Scheme S.1). Later, the *G* value rapidly increases between 45 and 60 s, since the number of radicals created on the PP surface increases together with the exposure time to UV light.

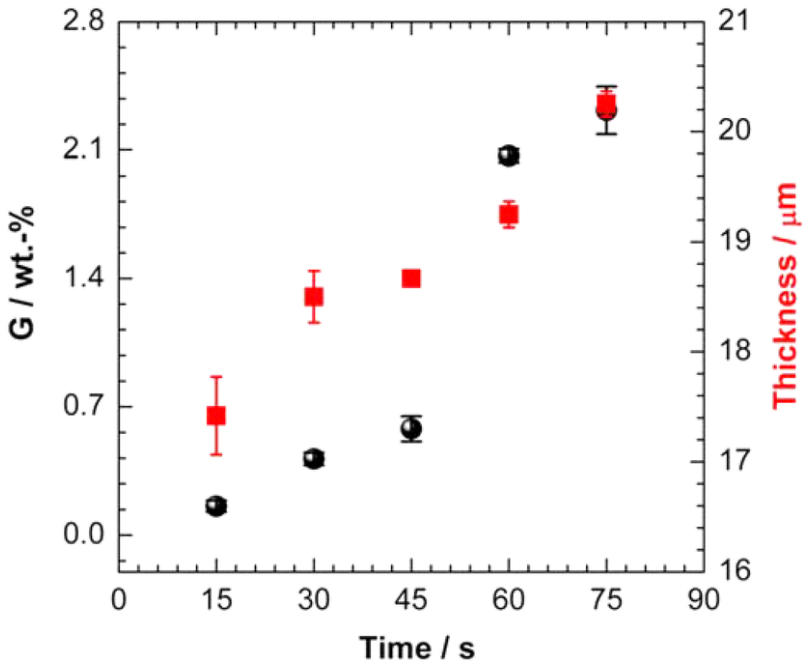

Figure 1 Influence of exposure time on *G* value (black) and thickness (red) when an AA-photograft polymerization on PP film takes place using a 0.10 M BP content.

After 60 s, the *G* value slightly changes, since almost all the monomer has already been consumed in the RM. In addition, a prolonged exposure time leads to the degradation of the surface PP chains, which results in low-molecular-weight oxides.[52] The initiation of AA homopolymerization is favored by these oxides, and competes with photograft polymerization. However, these free PAA chains were removed from the modified PP surface by exhaustively washing with aqueous NaOH solution. Considering the initial monomer content used in the RM and the *G* value reached (e.g., 2 wt %) for AA-photograft polymerization, it could be estimated that nearly 25 mol % of the monomers was grafted. Consequently, nearly 70 mol % or less of monomers became nongrafted PAA chains, and was eliminated together with unreacted AA by rinsing. Figure 1 also shows that the thickness of PAA-grafted PP films increases linearly upon longer exposure time, attributed to the growth of grafted PAA backbones and the increase in film surface roughness.[55] In addition, the surface of PP, PAA-grafted PP, and CS-adsorbed PP films was analyzed by attenuated total reflection infrared spectroscopy (ATR-FTIR). Figure 2 (left) shows that the most relevant bands of the initial PP film are attributed to C—H bond stretching vibration at 2925 and 2840 cm^{-1} and C—H bending vibration at 1456 and 1250 cm^{-1}. On the other hand, the surface of PAA-grafted PP film shows a new band near 1712 cm^{-1}, assigned to C=O stretching

vibration of the carboxyl group of PAA. It is also found that after AA-photograft reaction takes place onto the PP film surface, the characteristic signals of PP appear attenuated against the band of PAA carboxyl groups [Figure 2 (left)]. This behavior has been attributed to the fact that the PAA layer has been partially covered the PP surface. When a longer exposure time to UV light is used, the ratio of absorbance band from the carbonyl to the methylene group ($A_{1712\ cm\text{-}1}$/ $A_{1456\ cm\text{-}1}$) is increased [Figure 2 (right)].

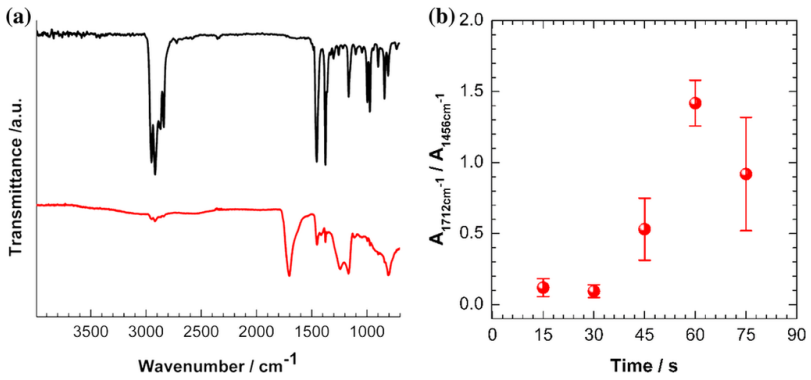

Figure 2 (Left) ATR-FTIR spectra of PP (black) and PAA-grafted PP (red) films obtained (2 wt % of *G* value) with 0.1 M BP concentration and 60 s of UV-radiation exposure time. (Right) Absorbance band ratio from carbonyl to methylene group ($A_{1712\ cm^{-1}} \Big/ A_{1456\ cm^{-1}}$) of PAA-grafted PP films prepared with 0.10 M of BP as a function of exposure time.

This ratio changes in a similar fashion to that of the *G* value shown in Figure 1, supporting the hypothesis explained above about the growth of PAA chains. In addition, at 75 s, the band ratio has a high error bar where this behavior is related to the fact that a greater degree of grafting leads to greater in-homogeneity and roughness in terms of the growth chain of grafted PAA.[55, 56] There is a reciprocal dependence between the *G* value and the distance from the lamp to a given area of the film.[55] The grafting degree on the film surface is accentuated mostly below the position of the lamp (smaller distance between the lamp and the film), while the *G* value decreases gradually as one moves toward the edges of the film. In addition, Supporting Information Figure S.1 (left) shows the effect of BP concentration on the performance of AA photograft reaction for 30 s of UV exposure. It can be seen that *G* value and thickness increase up to 0.10 M of BP concentration in a linear manner, and then, the curve profile tends to reach a plateau. This behavior can be attributed to the fact that the number of radicals created onto PP surface linearly increases with BP content until 0.10 M. Above this concentration, the number of active sites generated by hydrogen abstraction of BP onto surface of PP film is probably saturated and the growth of grafted PAA chains reaches a similar average value of length chains. Supporting Information Figure S.1 (right) also illustrates the variation in the absorbance band ratio of ($A_{1712\ cm\text{-}1}$/ $A_{1456\ cm\text{-}1}$) of the PAA-grafted PP film versus the concentration of the photoinitiator. This parameter shows a behavior similar to that found in Supporting Information Figure S.1 (left), which supports the fact that thickness depends on *G* values.

Synthesis and Adsorption of AgNP on PAA-Grafted PP Film

In this study, the effect of $AgNO_3$ concentration, such as a 5 or 30 mM, on the size distribution of the synthesized AgNP was examined. In this synthesis, a 1 wt % of CS and a silver-ion aqueous solution were mixed, and then thermally treated at 90 °C for 15 h.[46] The formation of AgNP in the RM was supported by the surface plasmon resonance (SPR) band measured by UV–Visible spectrophotometry. Figure 3 shows the spectra of $AgNP^5$/CS and $AgNP^{30}$/CS complexes in aqueous solution, characterized by a single and intense SPR band near 418 nm where the spectral features of AgNP synthesized in both cases are similar. However,

it is found that the maximum extinction measured with the $AgNP^{30}$/CS complex is about 4 times higher than that found for $AgNP^{5}$/CS.

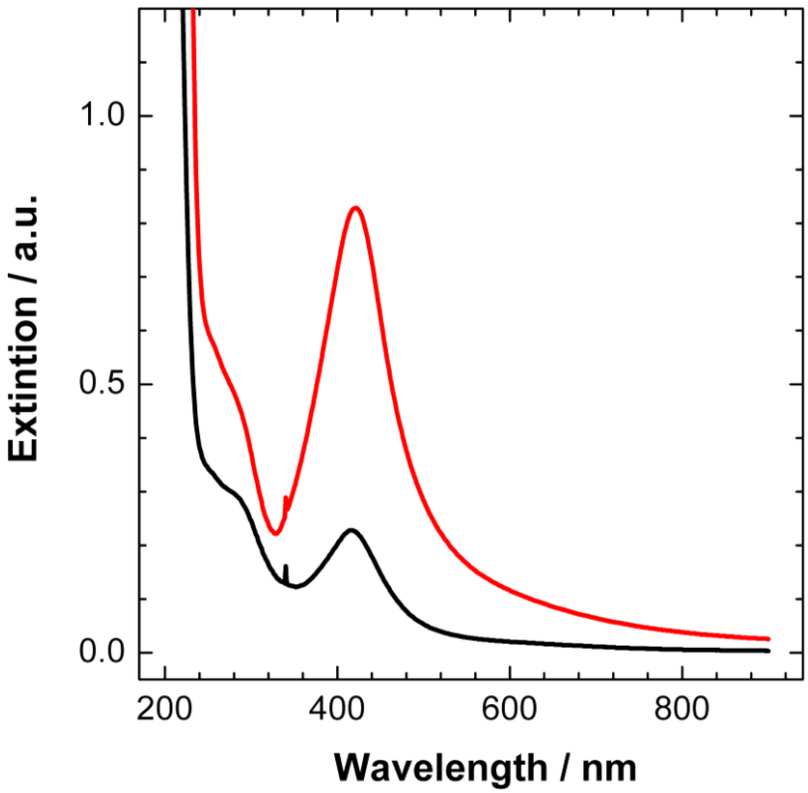

Figure 3 UV–visible spectral curves of $AgNP^{5}$/CS (black) and $AgNP^{30}$/CS (red) complexes synthesized.

This phenomenon is related to the fact that higher silver-ion concentration leads to the formation of a greater amount of AgNP with a smaller diameter. It is well known that the SPR band mostly depends on the AgNP shape and size distribution.[57, 58] During the formation of AgNP in the RM, two processes, such as nucleation and growth, take place. A high amount of small-diameter AgNP with a narrow distribution is generated from the nucleation reaction, whereas the growth process leads to the formation of AgNP with larger diameters and a wide-size distribution. In addition, the influence of $AgNO_3$ concentration on the AgNP size distribution of AgNP/CS complexes was characterized by TEM. Figure 4 shows the TEM micrographs of these complexes, where the morphology of AgNP looks like spheres. Figure 4 clearly exhibits that $AgNP^{30}$/CS complex yields a higher amount of smaller AgNP than that found for $AgNP^{5}$/CS.

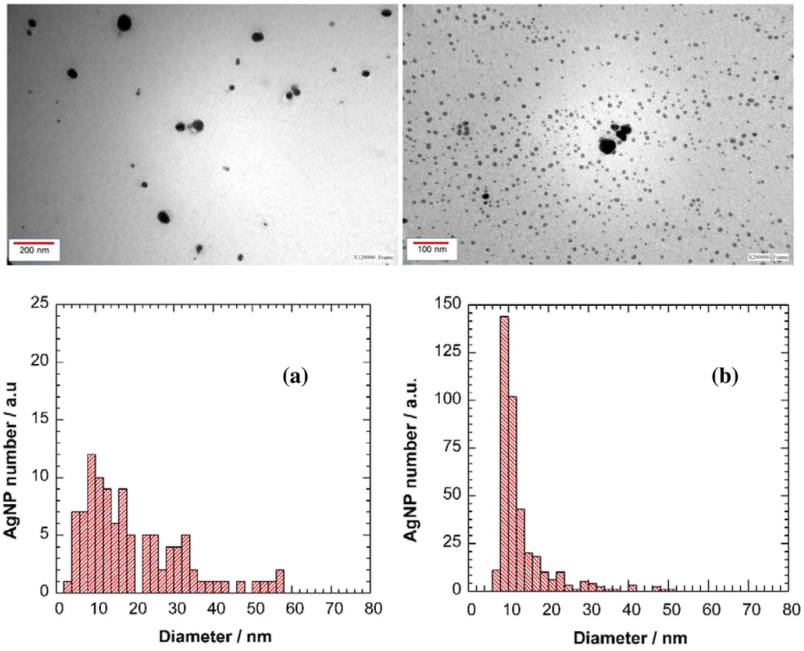

Figure 4 TEM Microphotographs (up) of $AgNP^{5}$/CS (left) and $AgNP^{30}$/CS (right) complexes synthesized from 5 and 30 mM of $AgNO_3$ aqueous solution, respectively, and their corresponding particle size distribution (down). A magnification of 120 and 200 kX and a size reference of 200 and 100 nm, respectively, were detailed inside.

Moreover, the size distribution of AgNP was obtained from the analysis of at least five TEM micrographs. Figure 4 shows that, in both cases, the maximum value of the AgNP size distribution is centered near 9 nm. However, the NP size distribution for the $AgNP^{30}$/CS complex has a higher AgNP number and is narrower than that found for $AgNP^{5}$/CS, and consequently, a higher specific surface area is expected. In relative terms, a higher silver-ion concentration gives a higher crosslinking degree of CS backbones by complexes formation with their amino groups. This process limits the diffusion of silver ions, so, the kinetics of the AgNP nucleation process is favored over growth. This predominance of the nucleation for $AgNP^{30}$/CS gives rise to the generation of a high amount of AgNP with a narrower size distribution and a smaller average diameter. Hence, the large specific surface area of these AgNP leads to a higher extinction value.[57, 58] Additionally, the AgNP content in the film was determined by a potentiometric assay,[44] which was nearly 0.02 and 0.08 wt % for $AgNP^{5}$/CS and $AgNP^{30}$/CS, respectively. Subsequently, AgNP/CS complexes were adsorbed on PAA-grafted PP films containing different *G* values, driven by the electrostatic interaction between the PAA carboxyl and CS amino groups.[52] The immobilization degree value (I) was calculated with eq. (2) from the mass variation of the products obtained ($AgNP^{x}$/CS-coated PP film) and is shown in Figure 5 as a function of BP concentration.

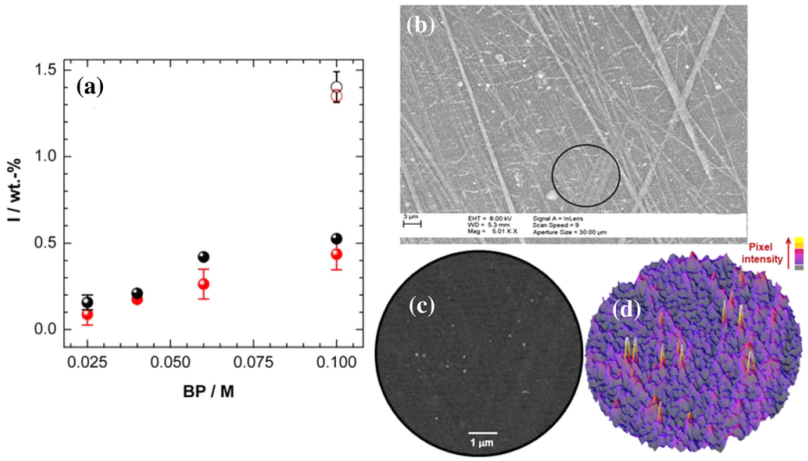

Figure 5 Immobilization degree (I) of AgNP^{5}/CS (red) and AgNP^{30}/CS (black) complex on PAA-grafted PP films obtained for 30 s (sphere) of UV radiation as a function of BP concentration or by exposure time of 60 s (circle) and 0.1 M of BP concentration (A). Error bars are sample standard deviations from quadrupled measurements. SEM micrographs of AgNP^{30}/CS-coated PP film obtained from secondary (B) and backscattered electrons detector (C), and the profile of pixel values (D) from the later.

It is found that the adsorption performance of the AgNP^{x}/CS complex directly depends on the content of the carboxyl groups on the film surface. PAA-grafted PP films synthesized from a higher BP content yield a higher I value; however, this trend is more pronounced for PAA-grafted PP films modified with an exposure time of 60 s. Figure 5 also shows that the I value for AgNP^{30}/CS-coated PP films is slightly higher than that exhibited for the AgNP^{5}/CS-coated PP film. This behavior is attributed to the fact that AgNP^{30}/CS complex contains an amount (mass and number) of smaller AgNP higher than that for AgNP^{5}/CS.

On the other hand, the surface morphology of AgNP/CS-coated PP films was characterized by SEM. Figure 5(A) and Supporting Information Figure S.2-left/up show that the surface of AgNP^{30}/CS-coated PP film has the formation of CS granules that are organized by forming cords, a typical arrangement pattern already described by Cavallo *et al.*[52] The comparison of the surface topography for both AgNP/CS-coated PP films determined from secondary electrons shows no significant differences between them [Figure 5(A) and Supporting Information Figure S.2-left/up]. This trend is consistent with the fact that the composition of the AgNP/CS complex contains mostly CS. Figure 5(B) and Supporting Information Figure S.2-right show white dots in a dark field, corresponding to the backscattered electrons from spheroidal AgNP, since Ag has an atomic number higher than that of C, N, and O (main components of the film). Figure 5(D) clearly shows the place where AgNPs are located in Figure 5(C) from the pixel signal. When comparing the AgNP/CS-coated PP film micrographs of backscattered electrons (Supporting Information Figure S.2-right/medium and down), a clear difference is found in the content of AgNP adsorbed on the surface for each film. As expected, the PP film containing AgNP^{30}/CS complexes exhibited a higher amount of smaller AgNP on the surface.

In addition, the adsorption of CS and AgNP^{x}/CS onto PAA-grafted PP films was also assessed by ATR-FTIR. Figure 6 (left) shows the spectral curves of CS-adsorbed PP, AgNP^{5}/CS-coated PP, and AgNP^{30}/CS-coated PP films. It is found that the CS-adsorbed PP film shows a new band at 1554 cm^{-1} corresponding to the N—H bending vibration, which decreases when CS amino groups interact with the AgNP surface for the AgNP^{x}/CS-coated PP film. This behavior agrees with the fact that the coordination complex limits the N—H vibrational mode and its intensity decreases.[28–32] The surface functional groups of AgNP^{x}/CS-coated PP films were also analyzed from the absorbance band ratio from the amino to the methylene group ($A_{1556\ \mathrm{cm}^{-1}} \Big/ A_{1456\ \mathrm{cm}^{-1}}$). Figure 6 (right) shows, that in most cases, the band ratio from N—H bending

vibration to C—H stretching mode for AgNP^{30}/CS-coated is lower than that for the AgNP^{5}/CS-coated PP film. Here, the signal of N—H bending vibration decreases by interaction between CS amino groups and AgNP surface, and reciprocally depends on the AgNP number, which supports that trend explained above. This band ratio is also associated with the content of AgNP/CS complexes adsorbed onto the PAA-grafted PP surface, where the N—H signal of CS is compared against C—H bending vibration, which mainly belongs to PP.

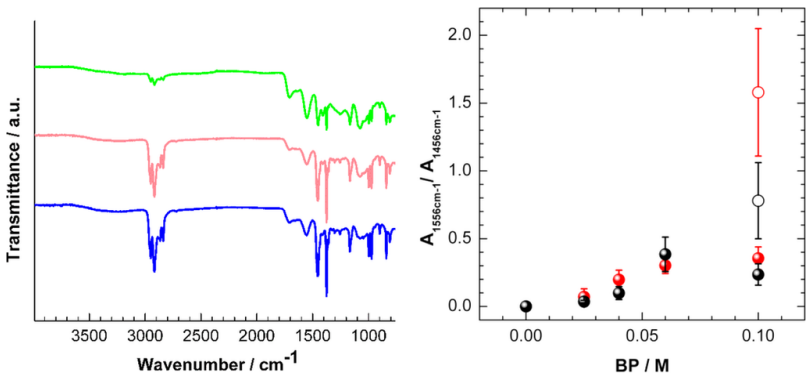

Figure 6 (Left) ATR-FTIR spectral curves of CS-adsorbed PP (green), AgNP^{5}/CS-coated (red), and AgNP^{30}/CS-coated PP (blue) films (I value near 1.4 wt %) obtained from PAA-grafted PP film (G = 2 wt %). (Right) Absorbance band ratio from amino to methylene group ($A_{1556\ cm\text{-}1}/A_{1456\ cm\text{-}1}$) of AgNP^{5}/CS (red) and AgNP^{30}/CS (black) complexes on PAA-grafted PP films, obtained for 30 s (sphere) of light exposure time as a function of BP concentration or 60 s (circle) of UV radiation.

Figure 6 (right) shows that this band ratio depends directly on the grafting degree of the PAA-grafted PP film, when BP content as well as grafting time are varied. This behavior was attributed to the fact that a higher content of carboxylate groups at the surface led to a higher adsorption of AgNP/CS complexes driven by electrostatic interaction with the ammonium groups of the CS chain. In addition, the error bar of the band ratio becomes significantly larger when the grafting degree increases, since roughness and inhomogeneity of film surface rise too.[51]

Active Surface Area of AgNP

Considering that the antimicrobial activity of AgNP depends on the average size as well as their shape, it was found that the specific surface area of a dose of AgNP increased when the average particle size decreased, yielding a more effective interaction of the material with the surrounding environment.[38] Therefore, a catalysis assay was carried out to demonstrate the AgNP surface activity of PP films to interact with different components. Here, the catalytic activity of AgNP adsorbed on the films was analyzed for the reduction reaction of 4-nitrophenol against $NaBH_4$ at 50 °C, using a 1:100 M ratio. Under these conditions, 4-nitrophenol was deprotonated and its conjugate base, sodium 4-nitrofenoxide, exhibited an absorption band at 400 nm. Supporting Information Figure S.3A shows the UV–Visible spectral curve of the RM supernatant. It is observed that the signal of sodium 4-nitrophenoxide decreases and the bands at 230 and 300 nm corresponding to sodium 4-amino-phenoxide increase when reduction reaction takes place. It was found that none of the films of AgNP^{5}/CS-coated (not shown) and AgNP^{30}/CS-coated PP films with a I value lower than 1 wt % showed catalytic activity for the reduction of 4-nitrophenol even after 5 h of reaction. This behavior was associated with the fact that the content of active AgNP on the surface was too low. Furthermore, when this reduction reaction was carried out without the presence of AgNP (CS-adsorbed PP film), the reduction of nitro-aryl group did not occur even after 20 h of reaction. Considering the fact that AgNP^{5}/CS-coated PP film has a AgNP content lower than that of the AgNP^{30}/CS-coated PP film, the reduction kinetics was followed only for the latter. Therefore, a AgNP^{30}/CS-coated PP film with a (22.5 ± 0.7) μm of thickness and an I value of (1.3 ± 0.1) wt % was obtained from adsorption of AgNP^{30}/CS complex onto a PAA-grafted PP film with

a (21 ± 1) μm thickness and a 2.1 wt % of *G* value (0.1 M of BP concentration and 60 s of UV irradiation). The catalytic performance was evaluated at 50 °C, demonstrating to be able to catalyze the reduction of 4-nitrophenol. Supporting Information Figure S.3B shows the performance of the $AgNP^{30}$/CS-coated PP film for the reduction kinetics of sodium 4-nitrophenoxide from the change of its extinction coefficient at 400 nm. Clearly, the catalytic action on the reduction reaction can be observed for three $AgNP^{30}$/CS-coated PP samples, which also supports the hypothesis of the existence of a minimum concentration of active AgNP on the film surface. An induction time of about 45 s was observed, where the O_2 molecules solubilized in the RM was adsorbed onto AgNP surface and consumed by the reaction with $NaBH_4$.[59] Afterward, the reduction reaction of sodium 4-nitrophenoxide took place, until this molecule was completely consumed close to 300 s. It should be noted that under these conditions, the reduction of 4-nitrofenol actually took place, indicating that AgNPs in the PP film have a surface active.

Antimicrobial Performance of AgNP/CS-Coated PP Films

Assay of Agar Disk Diffusion

The diameter of the inhibition zone was determined using the agar disk diffusion method after the incubation of a disk of the PP film with plates inoculated with either Gram-positive (*S. aureus*) or Gram-negative (*E. coli*) bacteria for 24 h at 37 °C. Supporting Information Figure S.4 shows the images of the plates with the disks, from which the inhibition zones were measured. Table 1 summarizes AMI values [eq. (3)]. Both AgNP/CS-coated PP films increased the inhibition zones against both strains when compared with the PP, PAA-grafted PP, and CS-adsorbed PP films.

Table 1 Agar Disk Diffusion Assay for PP-Based Films on an Inoculated Plate with Either S. aureus *or* E. coli for 24 h at 37 °C

Disk	*S. aureus* AMI (%)	*E. coli* AMI (%)
PP	0	0
PAA-grafted PP[a]	0	0
CS-adsorbed PP[b]	0	0
$AgNP^5$/CS-coated PP[b]	22 ± 5	27 ± 5
$AgNP^{30}$/CS-coated PP[b]	40 ± 5	32 ± 5

(a) Modified PP film (near 2 wt % of G value) obtained from 0.10 M of BP concentration and 60 s of UV-r adiation exposure time. (b) These films have an I value near 1.4 wt % and were obtained from<<Query: P lease confirm whether (a) and (b) represent table footnotes or general notes. Ans: They are table footnote s.>> PAA-grafted PP[a].

In addition, $AgNP^{30}$/CS-coated PP film shows higher AMI values than those found for $AgNP^5$/CS-coated PP film, which is related to the fact that the former has a larger amount of smaller AgNP with a higher specific surface area exposed to bacteria (Supporting Information Figure S.2). This result is in line with the behavior found for CS/cellulose films containing AgNP stabilized with polyacrylic acid reported by Li *et al.*, or for solid disks containing a 5 wt % of AgNP/bovine serum albumin together with bone cement informed by Valenti *et al.*[44, 60] Although these systems exhibited only antimicrobial activity nearly 1.6 times higher than that of $AgNP^{30}$/CS-coated PP film, the former contains a higher content of loaded AgNP. In addition, other authors

registered poorer antimicrobial activity for their AgNP-coated films than that found for the $AgNP^{30}$/CS-coated PP film.[61, 62] Finally, it is worth mentioning that Kuorwel *et al.*[54] indicated that films containing 0.50 wt % of natural antimicrobials (linalool, carvacrol, or thymol) showed a performance comparative with that of the $AgNP^{30}$/CS-coated PP film with particularly low AgNP content (0.08 wt %).

Growth and Viability of Planktonic Bacteria—Surface Colonization

The antimicrobial activity of AgNP/CS-coated PP films was evaluated by incubation with a liquid culture of *S. aureus* and *E. coli* to analyze the growth and viability of planktonic bacteria. The viable cell content was determined by the plate-counting method of the planktonic culture as a function of incubation time (Figure 7). In the first place, the films without AgNP showed the same behavior as those of control experiments (in the absence of films) for both strains. In addition, these profiles indicated a bacterial growth in the exponential phase at least during the first 6 h of incubation, where viable cell content rapidly increased until reaching a plateau at 10^9 CFU/mL after 24 h of incubation. On the other hand, noticeable differences arose for AgNP/CS-coated PP films against both strains. Figure 7 shows the number of viable cells for control and PP-films after 3, 6, 24, and 48 h of incubation with *S. aureus* (left panel) or *E. coli* (right panel). The logarithmic reduction on the viable cell content displayed in the same figure was calculated by comparing the bacterial content measured in culture incubated with AgNP/CS-coated PP films with those determined in the absence of AgNP (Supporting Information Table S.1). After 3 and 6 h of incubation with *S. aureus*, no significant differences were found between both AgNP/CS-coated PP films. In these conditions, bacterial growth was inhibited and the content of viable bacterial cells was maintained around the initial inoculum concentration. Hence, a logarithmic reduction between 1 and 3 log units was found. However, bacterial growth was recovered for $AgNP^5$/CS-coated PP film after 24 h of incubation with *S. aureus* until reaching the same content of viable bacteria measured with the films without AgNP (see also the effect on logarithmic reduction). In contrast, the $AgNP^{30}$/CS-coated PP film inhibited *S. aureus* growth up to more than 4 log units even after 48 h of incubation. Therefore, the trend observed for the $AgNP^5$/CS-coated PP film until 6 h of incubation shows only a delay in growth, while the $AgNP^{30}$/CS-coated PP film shows a strong effect on bacterial growth rate. A similar behavior was observed when performing the experiments with an initial inoculum concentration of 10^6 CFU/mL (Supporting Information Table S.2). On the other hand, viable *E. coli* cells were not detected for both AgNP/CS-coated PP films regardless of the incubation period. As a consequence, both AgNP/CS-coated PP films were highly effective in inducing bacterial death in the culture in contact with them. This effect is highlighted by the high logarithmic reduction, from 4.4 to 9.4, along incubation time (Supporting Information Table S.1).

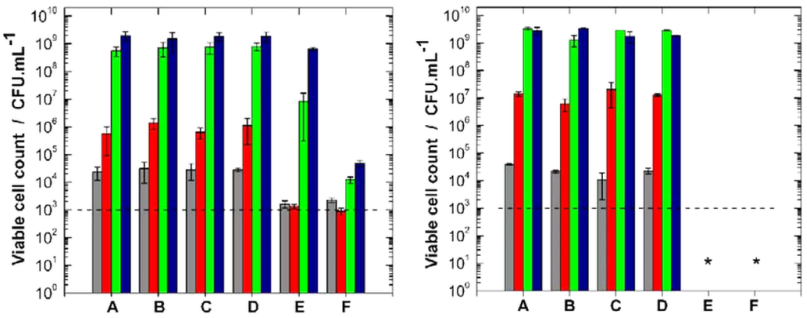

Figure 7 Antimicrobial performance of the PP (B), PAA-grafted PP with 2 wt % of *G* value (C), CS-adsorbed PP (D), $AgNP^5$/CS-coated PP (E), and $AgNP^{30}$/CS-coated PP films (F) with a I value close to 1.4 wt % against *S. aureus* (left) and *E. coli* (right) as a function of incubation time: 3 (gray), 6 (red), 24 (light green), and 48 h (navy blue). Initial inoculum concentration: 10^3 CFU/mL (represented with a dashed line). The symbol * indicates that viable cells were not detected in these cultures. The control experiment (A) was performed in the absence of the PP film.

Clearly, the AgNP^{30}/CS-coated PP film shows an excellent antibacterial performance for both strains even after long incubation periods. When these results are compared with those of other films with AgNP, the AgNP^{30}/CS-coated PP film shows a similar or better behavior, despite having lower NP content.[54, 63, 64]

Considering the weaker effect of AgNP/CS-coated PP films against *S. aureus*, surface colonization was also evaluated with this strain after 48 h of incubation, as shown in Figure 8. In general, poor *S. aureus* colonization can be observed on the modified-PP films in the absence of AgNP. However, bacterial colonization was completely inhibited on the AgNP^{30}/CS-coated PP film, highlighting that this film is also more efficient at inhibiting the bacterial colonization of the surfaces. The PP-coated film with the AgNP^{30}/CS complex shows a better antimicrobial performance than that found for the AgNP^{5}/CS-coated PP film since the former has a larger NP amount with a higher specific surface area. The active surface of the film modified with the AgNP^{30}/CS complex was previously demonstrated by the reduction reaction of 4-nitrofenol. It should be noted that the antibacterial performance of AgNP/CS-coated PP films resembles that of AgNP. Indeed, a recent work has shown that 10 nm of AgNP is more effective antibacterial agents than 50 nm ones, with a significantly higher susceptibility of *E. coli* than *S. aureus* to both NP size.[65] It was suggested that this difference in sensitivity might be due to the thickness of the cell walls, which is greater for Gram-positive (*S. aureus*) bacteria. This evidence supports the excellent performance of AgNP^{30}/CS-coated PP films, with a AgNP content as low as 0.08 wt %, in inhibiting bacterial growth and development under the conditions studied. This trend is consistent with an adequate amount of small AgNP adsorbed (1.5 μg cm^{-2}) in an organized manner within a thin surface layer (near 1 μm) on the film. This increase in the apparent AgNP concentration near the surface (estimated superficial content of 2 × 10^{-9} AgNP cm^{-2}) is the main cause of bacteria death under these conditions. These results turn this coating of film surface with AgNP as a more than promising strategy to be used in the preparation of antimicrobial surfaces.

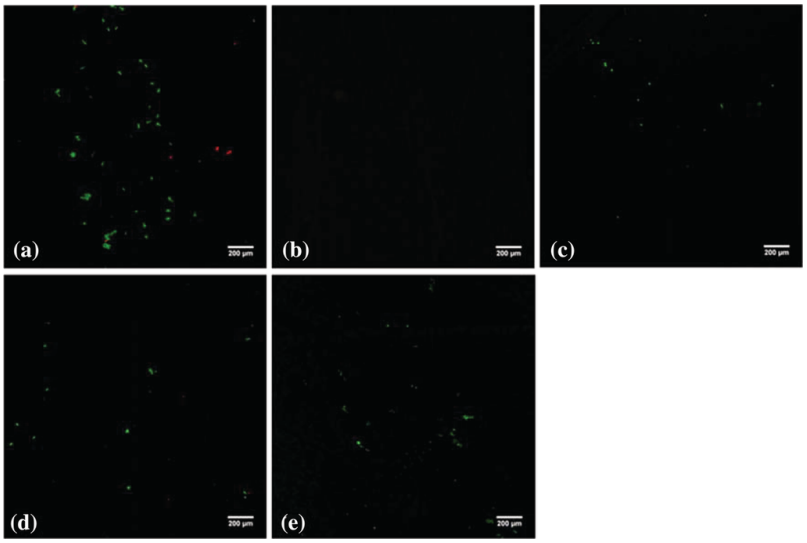

Figure 8 CLSM images after 48 h of growth of *S. aureus* on [a]AgNP**5**/CS-coated (A), [a]AgNP**30**/CS-coated PP film (B), PP (C), [b]PAA-grafted PP (D), and [a]CS-adsorbed PP films (E). Viable (green) and nonviable (red) bacteria are shown. (A) These films have an I value of nearly 1.4 wt % and were obtained from PAA-grafted PP[b]. (B) Modified PP film containing a 2 wt % of *G* value.

CONCLUSION

We evaluated the performance of AgNP/CS-coated PP films as active antimicrobial surfaces against *Staphylococcus aureus* and *Escherichia coli*. First, PP films were modified by photograft polymerization of AA.

AgNP were synthesized by thermal reduction of $AgNO_3$ against the functional groups of CS in order to prepare stabilized AgNP/CS complexes. Subsequently, the complexes were adsorbed onto the surface of PAA-grafted PP films driven by electrostatic interactions. Here, the remarkable role that CS has played in the synthesis and stabilization of AgNP and also as a binding agent for the surface should be noted. Later, the surface of the$AgNP^{30}$/CS-coated PP film showed a behavior against *S. aureus* better than that found for the $AgNP^{5}$/CS-coated PP film in terms of inhibition of bacterial growth and colonization, even at high initial planktonic cell concentration and long incubation periods. Moreover, the $AgNP^{5}$/CS-coated PP film was only capable of delaying the development of *S. aureus* growth at low initial inoculum concentration. On the other hand, the $AgNP^{30}$/CS-coated PP film showed a marked inhibition of *S. aureus* growth in all the conditions studied, decreasing more than 4 log units in the viable bacterial concentration after 48 h of incubation. This behavior is related to the higher specific surface area of AgNP in the $AgNP^{30}$/CS complexes as well as an adequate amount of small AgNP adsorbed in an organized manner within a thin surface layer close to 1 μm on the film. In brief, the good performance evidenced was related to the increase in the apparent AgNP concentration near the film surface. On the other hand, both AgNP-coated PP films were highly effective at inducing *E. coli* death in the culture in contact with them. This effect is highlighted by the high logarithmic reduction (from 4.4 to 9.4) along incubation time. The difference in sensitivity could be ascribed to the thickness of the cell walls, which is greater for Gram-positive (*S. aureus*) bacteria. Therefore, we believe that the antimicrobial activity of this film is particularly promising, and this work significantly contributes to the development of new strategies to prepare active surface for biomedical and food packaging materials.

ACKNOWLEDGMENTS

Giuliana Mosconi and María Fernanda Stragliotto thank CONICET for their doctoral and postdoctoral fellowship, respectively. In addition, the authors are grateful for the financial support received by CONICET from the projects PIP 11220110100499CO and PIP 11220150100344CO, FONCYT (PICT-2015-2477), and SeCyT-UNC (30820150100348CB). Authors also wish to acknowledge language assistance by Carolina Mosconi.

REFERENCES

[1] Xie, M.; Hu, B.; Wang, Y.; Zeng, X. *J. Agric. Food Chem.* 2014, **62**, 9128.

[2] Van Den Broek, L. A. M.; Knoop, R. J. I.; Kappen, F. H. J.; Boeriu, C. G. *Carbohydr. Polym.* 2015, **116**, 237.

[3] Epure, V.; Griffon, M.; Pollet, E.; Avérous, L. *Carbohydr. Polym.* 2011, **83**, 947.

[4] Amri, F.; Husseinsyah, S.; Hussin, K. *Compos. Part A Appl. Sci. Manuf.* 2013, **46**, 89.

[5] Ge, D.; Lee, H. K. *J. Chromatogr. A.* 2015, **1408**, 56.

[6] Pinto, R. J. B.; Fernandes, S. C. M.; Freire, C. S. R.; Sadocco, P.; Causio, J.; Neto, C. P.; Trindade, T. *Carbohydr. Res.* 2012, **348**, 77.

[7] Torlak, E.; Sert, D. *Int. J. Biol. Macromol.* 2013, **60**, 52.

[8] An, J.; Luo, Q.; Yuan, X.; Wang, D.; Li, X. *J. Appl. Polym. Sci.* 2011, **120**, 3180.

[9] Nedela, O.; Slepicka, P.; Svorcik, V. *Materials*. 2017, **10**, 1115.

[10] Gour, N.; Ngo, K. X.; Vebert-nardin, C. *Macromol. Mater. Eng*. 2014, **299**, 648.

[11] Kato, K.; Uchida, E.; Kang, E.; Uyama, Y.; Ikada, Y. *Prog. Polym. Sci.* 2003, **28**, 209.

[12] Ikada, Y. *Biomaterials*. 1994, **15**, 725.

[13] Li, Q.; Imbrogno, J.; Belfort, G.; Wang, X. *J. Appl. Polym. Sci.* 2015, **132**, 41781.

[14] Hu, S.; Brittain, W. J. *Macromolecules*. 2005, **38**, 6592.

[15] Zare, Y.; Rhee, K. Y.; Hui, D. *Compos. Part B Eng*. 2017, **122**, 41.

[16] Zhao, B.; Brittain, W. J. *Prog. Polym. Sci.* 2000, **25**, 677.

[17] Wang, H.; Ren, J.; Hlaing, A.; Yan, M. *J. Colloid Interface Sci.* 2011, **354**, 160.

[18] Wu, H.; Xiaohong, Z.; Huang, L.; Ma, L. F.; Liu, C. *Langmuir*. 2018, **37**, 11101.

[19] de Moraes Crizel, T.; de Oliveira Rios, A.; V. D. Alves, V.; Bandarra, N.; Moldão-Martins, M.; Hickmann Flôres, S. *Food Hydrocoll.* 2018, **74**, 139.

[20] Sadeghi-Kiakhani, M.; Safapour, S. *Fibers Polym*. 2015, **16**, 1075.

[21] Siripatrawan, U.; Vitchayakitti, W. *Food Hydrocoll.* 2016, **61**, 695.

[22] Madureira, A. R.; Pereira, A.; Castro, P. M.; Pintado, M. *J. Food Eng*. 2015, **167**, 210.

[23] Ramos, M.; Jiménez, A.; Peltzer, M.; Garrigós, M. C. *J. Food Eng*. 2012, **109**, 513.

[24] Abreu, A. S.; Oliveira, M.; De Sá, A.; Rodrigues, R. M.; Cerqueira, M. A.; Vicente, A. A.; Machado, A. V. *Carbohydr. Polym*. 2015, **129**, 127.

[25] Benhabiles, M. S.; Salah, R.; Lounici, H.; Drouiche, N.; Goosen, M. F. A.; Mameri, N. *Food Hydrocoll.* 2012, **29**, 48.

[26] Wang, L.; Liu, F.; Jiang, Y.; Chai, Z.; Li, P.; Cheng, Y.; Jing, H.; Leng, X. *J. Agric. Food Chem.* 2011, **59**, 12411.

[27] Cuervo-rodríguez, R.; López-fabal, F.; Gómez-garcés, J. L.; Muñoz-bonilla, A.; Fernández-garcía, M. *Macromol. Biosci.* 2017, **17**, 1700258.

[28] Banin, E.; Hughes, D.; Kuipers, O. P. *FEMS Microbiol. Rev.* 2017, **41**, 450.

[29] Luepke, K. H.; Suda, K. J.; Boucher, H.; Russo, R. L.; Bonney, M. W.; Hunt, T. D.; Mohr, J. F. *Pharmacotherapy*. 2017, **37**, 71.

[30] Mingeot-Leclercq, M.-P.; Décout, J.-L. *Med. Chem. Commun.* 2016, **7**, 586.

[31] Türkan, F.; Huyut, Z.; Taslimi, P.; Gülçin, İ. *Arch. Physiol. Biochem.* 2018, **351**, 1800200.

[32] Zimmermann, L.; Das, I.; Désiré, J.; Sautrey, G.; Vinicius Barros, R. S.; El Khoury, M.; Mingeot-Leclercq, M. P.; Décout, J. L. *J. Med. Chem.* 2016, **59**, 9350.

[33] Laht, M.; Karkman, A.; Voolaid, V.; Ritz, C.; Tenson, T.; Virta, M.; Kisand, V. *PLoS One*. 2014, **9**, 103705.

[34] Mölstad, S.; Löfmark, S.; Carlin, K.; Erntell, M.; Aspevall, O.; Blad, L.; Hanberger, H.; Hedin, K.; Hellman, J.; Norman, C.; Skoog, G.; Stålsby-Lundborg, C.; Tegmark Wisell, K.; Åhrén, C.; Cars, O. *Bull. World Health Organ.* 2017, **95**, 764.

[35] Rex, J. H.; Talbot, G. H.; Goldberger, M. J.; Eisenstein, B. I.; Echols, R. M.; Tomayko, J. F.; Dudley, M. N.; Dane, A. *Clin. Infect. Dis.* 2017, **65**, 141.

[36] Applerot, G.; Lellouche, J.; Perkas, N.; Nitzan, Y.; Gedanken, A.; Banin, E. *RSC Adv.* 2012, **2**, 2314.

[37] Haussler, S.; Fuqua, C. *J. Bacteriol.* 2013, **195**, 2947.

[38] Markowska, K.; Grudniak, A. M.; Wolska, K. I. *Acta Biochim. Pol.* 2013, **60**, 523.

[39] Kumar, R.; Münstedt, H. *Biomaterials*. 2005, **26**, 2081.

[40] Nguyen, V. H.; Kim, B. K.; Jo, Y. L.; Shim, J. J. *J. Supercrit. Fluids*. 2012, **72**, 28.

[41] Jazayeri, M. H.; Aghaie, T.; Avan, A.; Vatankhah, A.; Ghaffari, M. R. S. *Sens. Biosensing Res.* 2018, **20**, 1.

[42] Lismont, M.; Dreesen, L.; Wuttke, S. *Adv. Funct. Mater*. 2017, **27**, 1.

[43] Priyadarshini, E.; Pradhan, N. *Sens. Actuators B Chem*. 2017, **238**, 888.

[44] Valenti, L. E.; Giacomelli, C. E. *J. Nanopart. Res*. 2017, **19**, 156.

[45] Wei, D.; Qian, W. *Colloids Surf. B Biointerfaces*. 2008, **62**, 136.

[46] Wei, D. W.; Sun, W. Y.; Qian, W. P.; Ye, Y. Z.; Ma, X. Y. *Carbohydr. Res*. 2009, **344**, 2375.

[47] Shao, W.; Liu, X.; Min, H.; Dong, G.; Feng, Q.; Zuo, S. *ACS Appl. Mater. Interfaces*. 2015, **7**, 6966.

[48] Cockerill, F.; Wickler, M.; Alder, J. *USA*. 2012, **32**, 188.

[49] Kumar, M. N. V. R. *React. Funct. Polym*. 2000, **46**, 1.

[50] Rinaudo, M. *Prog. Polym. Sci*. 2006, **31**, 603.

[51] Stragliotto, M. F.; Gomez, C. G.; Mosconi, G.; Strumia, M. C.; Romero, M. R. *Sens. Actuators B*. 2018, **277**, 78.

[52] Cavallo, J. A.; Gomez, C. G.; Strumia, M. C. *Macromol. Chem. Phys*. 2010, **211**, 1793.

[53] Balouiri, M.; Sadiki, M.; Ibnsouda, S. K. *J. Pharm. Anal*. 2016, **6**, 71.

[54] Kuorwel, K. K.; Cran, M. J.; Sonneveld, K.; Miltz, J.; Bigger, S. W. *J. Food Sci*. 2011, **76**, M531.

[55] Stragliotto, M. F.; Strumia, M. C.; Gomez, C. G.; Romero, M. R. *Ind. Eng. Chem. Res*. 2018, **57**, 1188.

[56] Costamagna, V.; Wunderlin, D.; Larran, M.; Strumia, M.; Herriko, E.; Europa, P.; Sebastian, D. *J. Appl. Polym. Sci.* 2006, **102**, 2254.

[57] Coronado, E. A.; Encina, E. R.; Stefani, F. D. *Nanoscale*. 2011, **3**, 4042.

[58] Douglas-Gallardo, O. A.; Gomez, C. G.; Macchione, M. A.; Cometto, F. P.; Coronado, E. A.; Macagno, V. A.; Pérez, M. A. *RSC Adv*. 2015, **5**, 100488.

[59] Panigrahi, S.; Basu, S.; Praharaj, S.; Pande, S.; Jana, S.; Pal, A.; Ghosh, S. K.; Pal, T. *J. Phys. Chem. C*. 2007, **111**, 4596.

[60] Lin, S.; Chen, L.; Huang, L.; Cao, S.; Luo, X.; Liu, K. *Ind. Crops Prod*. 2015, **70**, 395.

[61] Salari, M.; Khiabani, M. S.; Mokarram, R. R.; Ghanbarzadeh, B.; Kafil, H. S. *Food Hydrocoll.* 2018, **84**, 414.

[62] Spagnol, C.; Fragal, E. H.; Pereira, A. G. B.; Nakamura, C. V.; Muniz, E. C.; Follmann, H. D. M.; Silva, R.; Rubira, A. F. *J. Colloid Interface Sci.* 2018, **531**, 705.

[63] Regiel, A.; Irusta, S.; Kyzioł, A.; Arruebo, M.; Santamaria, J. *Nanotechnology*. 2013, **24**, 015101.

[64] Penchev, H.; Paneva, D.; Manolova, N.; Rashkov, I. *Macromol. Biosci.* 2009, **9**, 884.

[65] Kubo, A.-L.; Capjak, I.; Vrcek, I. V.; Bondarenko, O. M.; Kurvet, I.; Vija, H.; Ivask, A.; Kasemets, K.; Kahru, A. *Colloids Surf. B Biointerfaces*. 2018, **170**, 401.